Transition from insulator to superconductor and significant enhancement of superconductivity in FeSe films via tuning Fe-vacancy disorders

Wenbin Qiu[2], Zongqing Ma[1, 2*], Yongchang Liu[1], Xiaolin Wang[2], Shi Xue Dou[2]

[1] –*Tianjin Key Laboratory of Composite and Functional Materials, School of Materials Science & Engineering, Tianjin University, Tianjin 300072, People's Republic of China*

[2] –*Institute for Superconducting and Electronic Materials, AIIM, University of Wollongong, Squires Way, North Wollongong, NSW 2500, Australia*

Abstract:

In contrast to its bulk crystals, the FeSe film or layer exhibits better superconductivity performance, which attract much interest in its fundamental research as well as potential application. Especially, the dominant factor and the exact enhancement mechanism of superconductivity need to be clarified in these systems. In present work, transition from insulator to superconductor and significant enhancement of superconductivity were achieved in the high quality (*00l*) oriented FeSe films via controlling the thickness as well as the Fe/Se ratio. The highest T_c up to 15.2 K (almost 2 times higher than those of bulk crystals) and H_{c2} up to 35.5 T are obtained in our atmosphere-stable FeSe thin film with practical thickness (240 nm), implying their great potential application in the electronic devices at high magnetic fields. More importantly, it was found that the Fe-vacancy disorder in FeSe films is the intrinsic factor determining the evolution of the superconductivity, rather than thickness effect.

* Corresponding author E-mail: mzq0320@163.com

In our non-superconducting FeSe film with Fe/Se ratio of 1.00:1.09, insulating β-$Fe_{1-x}Se$ phase with iron-vacancy disorders is the main phase and more likely to be the parent phase of FeSe superconducting system. Tuning the Fe-vacancy disorders via changing the Fe/Se ratio can dramatically vary the concentration of charge carrier and introduce proper electron doping, which finally leads to the transition from insulator to superconductor and further enhancement in the superconductivity. Intriguingly, our results also indicate that when the Fe/Se ratio of film is beyond a critical value, superconducting FeSe films will become instable, and phase separation occurs with new non-superconducting phase precipitating in the superconducting matrix, causing the degradation in the superconductivity. The results in present work help us to well understand the intrinsic mechanism of superconductivity among Fe-Se superconducting system and provide a new strategy to further pursue higher T_c in these materials.

Keywords: FeSe film; Fe-vacancy disorder; T_c

1. Introduction

The discovery of iron-based materials with a high superconducting transition temperature *Tc* has attracted much attention for both fundamental studies and practical applications [1]. Till now, plenty of efforts have been made to obtain higher superconducting performance, but the intrinsic mechanism of superconductivity in these systems is still being explored. Among iron-based superconducting family, the Iron selenide (FeSe) has the simplest structure with binary chemical composition, consisting of only two-dimensional conducting planes [2], rendering it to be an appropriate candidate for exploring the intrinsic mechanism of iron-based superconductors.

Compared with bulk crystals, FeSe in the form of film or multilayer attracts more attention as large enhancement in superconducting performance is obtained. Especially, recently high T_c (around 77K) was reported in single unit-cell FeSe layer [3], which is considered as the highest value among all the iron-based superconductors. As for the enhancement mechanism of superconductivity in FeSe film or layer, there is still a hot debate and research groups around the world have proposed various viewpoints such as internal pressure effect [4], interface effect [5, 6] and other thickness-related effects. Thus more fundamental work is still required to understand the superconductivity of FeSe films and multilayer in depth. What's more, an interesting physical phenomenon, the superconductor-insulator transition (SIT) is also found in the FeSe film [7]. Various parameters might induce SIT, and clearly transitions were found by tuning disorder [7, 8] or magnetic field [9, 10]. Till now the

underlying mechanism of SIT is still under controversy. Clarifying the nature of SIT in FeSe film can provide a valuable hint to reveal the intrinsic mechanism of superconductivity in FeSe system.

On the other hand, a very important question that whether we can realize a very high T_c in the bulk nature (for example, films) as that in single unit-cell FeSe layer is also raised. In contrast to the instability of FeSe single layer or multilayer in atmosphere, FeSe thin film can be stable in atmosphere at room temperature and thus could act as a satisfying media for various characteristics or physical measurements to explore the nature of iron based superconductors. Moreover, high quality FeSe films with higher T_c and H_{c2} have a broad application prospect in the electronic devices at ultrahigh magnetic field. However, due to the very narrow homogeneity range of the β-FeSe superconducting phase and the coexisting impurity phases of Fe and Fe_7Se_8 [11], the preparation of high quality FeSe films with practical thickness is not an easy case. So far several methods are attempted to fabricate FeSe thin films, including pulsed laser deposition (PLD) [12, 13], sputtering [14] and molecular beam epitaxy (MBE) [15]. However, the T_c in these fabricated FeSe film are rather low, and there are few reports on the fabrication of stable FeSe thin films with good superconducting properties.

In present work, high quality (*00l*) oriented FeSe thin films were fabricated by PLD via optimizing processing parameters as well as controlling Fe/Se ratio. Clear SIT phenomenon and significant improvement in T_c (up to 15.2 K) and H_{c2} (up to 35.5 T) were found in these atmosphere-stable FeSe thin films with practical thickness. According to our investigation, the Fe-vacancy disorder in FeSe films is the intrinsic

factor determining the SIT and the evolution of the superconductivity, rather than other thickness-related factors. Tuning the Fe-vacancy disorders via changing the Fe/Se ratio in FeSe films can vary the concentration of electron carrier and introduce proper electron doping, which can lead to the transition from insulator to superconductor and further enhancement in the superconductivity. It was also found that there is a critical Fe/Se ratio for the stability of superconducting FeSe films. When the Fe/Se ratio of film is beyond this critical value, phase separation will occur in the film and new non-superconducting phase will gradually precipitate in the superconducting matrix, degrading the superconductivity performance.

2. Experimental

FeSe thin films are deposited by PLD (Nd: YAG, wavelength: 355 nm, 10 Hz as repetition rate, 2 Watt as output power) method under a high vacuum level better than 5×10^{-4} Pa. CaF_2 (100) single crystal with lattice parameter a = 5.462 Å ($\frac{a}{\sqrt{2}} = 3.862$ Å) is selected as growing substrate because the mismatch compared with *a*-axis parameter of FeSe film (a ≈ 3.8 Å) is very small. Home-made FeSe pellet was served as target, which was made from commercial available Fe and Se powder with a nominal composition by standard two step solid state sintering. By controlling the deposition time, FeSe films with thicknesses of 40 nm, 120 nm, 240 nm and 360 nm (denoted as #NS1, #SC1, #SC2 and #SC3, respectively) are obtained at 300 ˚C. The X-ray diffraction (XRD) is applied to characterize the crystal structure of FeSe films. Scanning electron microscopy (SEM, JEOL JSM-6490LV) equipped with high-accuracy EDX detector is employed to check the morphology information and

chemical composition of these prepared films, while field emission scanning electron microscopy (FESEM, JEOL JSM-7500) is used to obtain high-resolution images. Both of the electrical resistivity and Hall measurements under different magnetic fields were carried out on a 9T physical property measurement system (PPMS).

3. Results and discussion

The electronic resistivity versus temperature dependence (R-T curves) is illustrated in Figure 1(a). With increasing thickness from 40 nm to 240 nm, clear insulator-superconductor transition and gradually enhancement of superconductivity is observed. Interestingly, the superconductivity performance is suppressed when the thickness of FeSe films further increases from 240 nm to 360 nm. The highest T_c^{onset} up to 15.2 K and T_c^{zero} up to 13.5 K are obtained in the film sample with thickness of 240 nm (#SC2), which is about 2 times higher than that in FeSe polycrystalline bulks. This is the first time to achieve such high temperature superconductivity in FeSe film with practical thickness without introducing either epitaxial interface or external pressure. Moreover, this high-quality film is quite stable in atmosphere and potentially employed to various characteristics and properties measurement.

Full range R-T data from room temperature to 4.2K for these FeSe films is plotted in the inset of Fig 1(a), showing absolutely different temperature dependences: for FeSe film with thickness about 40 nm (#NS1), insulator-like behavior is appeared especially below 50K, and for the other films which are 3, 6 and 9 times thicker, their R-T curves behave in a metallic way, implying that qualitative change occurs in the structure of energy band, which will be discussed in detail later. In order to further

investigate the upper critical magnetic field (H_{c2}) of our films, measurements of R-T are executed by applying different magnetic fields, and such an example is shown in Fig 1(b). The transition shifts to lower temperatures under higher field and ΔT_c gets wider, which is a common characteristic in type-II superconductors. $H_{c2}(0)$ is determined by linear extrapolation fitting of T_c^{mid}, as shown in Fig 1(c). The estimated H_{c2} in three superconducting FeSe films are about 27.8 T, 35.5 T and 31.5 T for 120 nm, 240 nm and 360 nm respectively, and the highest $H_{c2}^{240\ nm} \approx 35.5$ T obtained in our work is a competitive candidate for world record in FeSe superconducting films. Excellent T_c and H_{c2} obtained in the atmosphere-stable FeSe films with practical thickness prepared in our work imply their great potential application in the electronic devices at ultrahigh magnetic fields. More importantly, understanding the underlying mechanism of SIT and significant enhancement of superconductivity observed in our FeSe films could provide meaningful hint for exploring the intrinsic mechanism of unconventional iron-based superconductors and shed light on further pursuit of higher T_c in these materials.

Since the evolution of superconductivity in the FeSe films is close related to the thickness, simply superficial conclusion that some thickness-related factors, such as anisotropic stress, transfer of carrier from substrate and epitaxial interface effect, play key role in the evolution of superconductivity could be easy to make in previous studies [4-6]. Nevertheless, further systemically investigations on chemical composition, lattice distortions, hall coefficient and microstructure in the FeSe films prepared in present work strongly point out that actually the modulation of the Fe/Se

ratio or the concentration of Fe-vacancy disorders is the intrinsic factor determining the SIT and the evolution of the superconductivity, rather than thickness-related factors mentioned above. Detailed information of four prepared FeSe films are listed in Table 1, including film thickness, superconducting performance, elements ratio of Fe/Se, lattice parameter, etc. It is worth noting that the chemical compositions (denoted as Fe:Se) of four prepared FeSe films are different with 1.00:1.09 for $FeSe_{40\ nm}$, 1.00:1.03 for $FeSe_{120\ nm}$, 1.00:1.04 for $FeSe_{240\ nm}$, 1.00:1.06 for $FeSe_{360\ nm}$, implying that all of them contain some Fe-vacancy disorders. These results will strongly support and give reference to our following discussion on the superconductivity mechanism.

Typical XRD patterns of four FeSe films are displayed in Fig 2(a) ranging from 10 to 80 degree. Well *c*-axis oriented texture is indexed based on PbO tetragonal structure in all samples, except for the spectrum of #NS1 in which the diffraction peaks of film are blurry due to poor crystallization. As illustrated in Fig 2(b), fine analysis on XRD spectrum is carried out by magnifying the interval between 15.5° and 17.0°. When film gets thicker, increase in peak intensity and monotonous peak shifting toward lower angle are both recognized, demonstrating that not only better crystallization and more grains preferring out-of-plane texture derive, but also some lattice distortion takes place. Lattice parameter *c* is calculated based on these XRD data and presented in table. 1. One can see that except non-superconducting film (#NS1), *c* in all the FeSe films (#SC1, #SC2 and #SC3) is larger than that for bulk single crystals, and increased significantly as thickness increasing. Since the difference between the

lattice constants of the CaF_2 substrate and FeSe overlayer is very small, it cannot be simply attributed to the lattice mismatch. Combined with EDX results mentioned above, the change in the Fe/Se ratio should be responsible for this evolution of lattice parameter and corresponding shift of diffraction peak position. Generally, the lower Fe/Se ratio means more Fe-vacancy disorders in the films, causing the elongation in parameter *c* and thus the corresponding position of β-FeSe (00l) diffraction peaks is supposed to locate at the lower angle.

On the other hand, compared to other superconducting films, obvious shift toward higher angle of the peak locating between 15.5˚ and 17˚ in the film #NS1 is abnormal, considering that its Fe/Se ratio is 1:1.09, much lower than other films. It is explained that the Fe/Se ratio of #NS1 film exhibits Se-excess as high as 9% compared with stoichiometric composition, which is far out of the range in which FeSe shows superconductivity given by McQueen et al [16]. In good accordance with Chen et al's work [17], one type of iron-vacancy disorder β-$Fe_{1-x}Se$ phase could exist in this FeSe film as the main phase rather than superconducting β-FeSe phase. The diffraction peaks of #NS1 film should origin from this type of β-$Fe_{1-x}Se$ phase and thus exhibit different diffraction peak position from β-FeSe phase. In Chen et al's work [17], they found that this β-$Fe_{1-x}Se$ phase with particular iron-vacancy disorder shows insulator behavior in R-T dependence, also quite consistent with our result shown in Fig. 1. They also proposed that this phase is more likely to be parent phase of FeSe superconducting system instead of the previously assigned β-$Fe_{1+\delta}Te$ phase. More

discussion on this speculation will be carried out later based on our analysis of hall coefficient.

Hall coefficient (R_H) is calculated by sweeping the magnetic field at fixed temperature, as shown in Fig. 3. R_H is the slope of Hall transverse resistivity ρ_{xy} at designated field B (> 1 T), determined as $R_H = \rho_{xy}/B$. All the superconducting FeSe films prepared in our work have negative R_H throughout the whole range, indicating electrons serve as the dominant charge carriers. In the R_H of three films showing superconductivity, common tendency can be observed that R_H keeps almost constant at temperature range higher than 100 K, then the absolute value of R_H increases with different acceleration depending on monotonous diminishing of film thickness, which is a strong evidence for the multiband nature in FeSe 11 system. The carrier concentration n is denoted via $n = 1/(qR_H)$ where q is the carrier charge. Obviously observed from Fig 3, higher electron carrier concentration is found at thicker FeSe superconducting film with more Fe vacancy disorders, which is opposite to the general concept that Fe vacancy disorders are supposed to introduce hole charge carriers, and the more Fe vacancy disorders, the more hole charge carriers. This abnormal phenomenon is probably attributed to the disorder-induced 'effective Fe self-doping', derived from Fe vacancy disorders enlarging electron pockets, which has been systematically analyzed by Berlijn's group [18].

In the case of sample #NS1, some fluctuation is observed in R_H value which is probably due to the poor response of transport R_{xy} signal detected in insulator-like FeSe film. As temperature goes down from room temperature to 50K, R_H slightly

increases at minus side and exhibits a broad peak at about 50 K. Then the absolute value of R_H steeply decrease and even reaches the value above 0 as temperature further goes down from 50K to 20K. R_H value changing from negative to positive at low temperature means that the dominant charge carriers change from electrons to holes in this non-superconducting FeSe film. The electron concentration hits a lower bound near 50 K and the inflection point in Hall measurement is in good agreement with R-T dependence where the resistivity of sample #NS1 shows a significant upturn after 50 K. Comparing our results with others' work, similar R_H-T curve has been published in $BaFe_2As_2$ system [19] and annealed single-unit-cell FeSe film [6], in which typical superconductivity is detected. Hence, we predict that insulator behavior in our 40 nm thick non-superconducting FeSe film is induced by the transformation in electronic state at 50 K, and superconductivity is supposed to emerge once this transformation is suppressed by introducing more electron charge carrier. Actually, in Chen et al's work [17], they proposed that an insulating β-$Fe_{1-x}Se$ phase with particular iron-vacancy disorder in Fe-Se system could be the parent phase of FeSe superconducting system instead of β-$Fe_{1+\delta}Te$ phase. Our results here are quite consistent with their prediction. As discussed above, β-$Fe_{1-x}Se$ phase with iron-vacancy disorders is the main phase in our non-superconducting FeSe film, which brings about the insulator-like behavior in R-T curve and abnormal change in the R_H-T curve, and can serve as parent phase of FeSe superconducting system. As the thickness of FeSe film increases from 40 nm to 120 nm in our work, the iron-vacancy disorders are tuned accompanying with the change in the Fe/Se ratio and electron

charge carriers are introduced (see the R_H in the Fig. 3), prompting the transition from insulator to superconductor and superconducting phase starts to domain in sample #SC1. With Fe/Se ratio is further changed in the thicker FeSe film #SC2, more electron carriers are introduced, which leads to the enhancement of superconductivity in this film. Besides tuning the internal Fe-vacancy disorder, recently other methods including alkali metal doping [20] and liquid-gating technique [21] were employed to introduce the electron carrier concentration in the FeSe multilayer or films with aim of achieving SIT and enhancing superconductivity. What's more, in our latest work, excellent superconductivity is also observed in the FeSe film with 40 nm thick (#NS1) by depositing Mg coating layer that can introduce proper amount of electron carrier. All these similarities offer strong verification to our speculation discussed above, and also hint a possibly universal underlying physics in these heavily electron doped FeSe superconductors. It is worth noting that the FeSe film with lowest Fe/Se ratio can introduce more electron carriers (see R_H-T curve in Fig. 3) and should exhibit the best superconductivity according to our speculation above. However, slight degradation in T_c and H_{c2} in the thickest film #SC3 suggests some other negative factors might suppress the superconducting performance.

In order to clarify the underlying degradation mechanism of superconductivity in film #SC3, the morphology of FeSe films #SC2 and #SC3 is observed by FESEM and presented in Fig 4(a) and 4(b), respectively. Flat and homogeneous surface is observed in Fig 4(a) with only sporadic Fe-rich particles (determined by EDX analysis) emerge. On the other hand, massive tiny particles homogenously precipitate

within the matrix of thickest film #SC3, as illustrated in Fig 4(b). Compared with big Fe-rich particles in the film #SC2, those precipitates are in absolutely different shape and distributed ultra-uniformly on the whole surface of FeSe film #SC3 (see enlarged image in Fig 4(c)). From the EDX investigation, their Fe/Se ratio is around 1.00:0.80, classifying them as another kind of Fe-rich phase. These emerging precipitates might be non-superconducting and magnetic, and can have negative impact on superconductivity. Consequently, superconducting performance of film #SC3 is slightly suppressed with lower T_c and H_{c2} compared to film #SC2. The presence of these unique precipitates explains well the abnormalities in the superconductivity and R_H performance of film #SC3, with respect to our proposed speculation. The evolution in the morphology of FeSe films observed here accompanying with change in Fe/Se ratio also implies that there is a critical Fe/Se ratio for the stability of superconducting FeSe films. When the Fe/Se ratio of film is beyond this critical value, phase separation will occur in the film even if its thickness is comparable small (in our case, the thickness is only 360 nm), and new non-superconducting phase will precipitate in the superconducting matrix, degrading the superconductivity performance. Further research focusing on the formation mechanism, characterization and electromagnetic properties of these precipitates need to carried out in terms of their affect on the superconductivity of FeSe.

4. Summary and conclusion

In summary, high quality (*00l*) oriented FeSe thin films on CaF_2 (100) substrate were fabricated by PLD via optimizing processing parameters as well as Fe/Se ratio. Clear

SIT phenomenon and significant enhancement of superconductivity were found in these FeSe thin films. The highest T_c up to 15.2 K and H_{c2} up to 35.5 T, almost twice than that of bulk crystals, are obtained in our atmosphere-stable FeSe thin film with practical thickness, implying their great potential application in the electronic devices at high magnetic fields. According to our investigation, the Fe-vacancy disorder in FeSe films is the intrinsic factor determining evolution of the superconductivity, rather than thickness effect. In our non-superconducting FeSe film, β-$Fe_{1-x}Se$ phase with iron-vacancy disorders is the main phase, which brings about the insulator-like behavior in R-T curve, and could serve as parent phase of FeSe superconducting system. Tuning the Fe-vacancy disorders via changing the Fe/Se ratio in these films can vary the concentration of charge carrier and introduce proper electron doping, which finally leads to the transition from insulator to superconductor and further enhancement in the superconductivity. It was also found that when the Fe/Se ratio of film is beyond a critical value, superconducting FeSe films will become instable, and phase separation occurs with new non-superconducting phase gradually precipitating in the superconducting matrix, causing the degradation in the superconductivity. These results will provide meaningful hint for exploring the intrinsic mechanism of unconventional iron-based superconductors and open a promising way for further pursuit of higher T_c in these materials.

Acknowledgement *This work is supported by the Australian Research Council (Grant No. DE140101333). The authors are also grateful to the China National Funds for Distinguished Young Scientists (Grant No. 51325401) and National Natural*

Science Foundation of China (Grant No. 51302186 and 51574178). The authors acknowledge use of facilities within the UOW Electron Microscopy Centre.

References

[1]. Y. Kamihara, T. Watanabe, M. Hirano, and H. Hosono, J. Am. Chem. Soc. 130, 3296 (2008).

[2]. F. C. Hsu, J. Y. Luo, K. W. Yeh, T. K. Chen, T. W. Huang, P. M. Wu, Y. C. Lee, Y. L. Huang, Y. Y. Chu, D. C. Yan, and M. K. Wu, Proc. Natl. Acad. Sci. U.S.A. 105, 14262 (2008).

[3]. Q. Y. Wang, Z. Li, W. H. Zhang, Z. C. Zhang, J. S. Zhang, W. Li, H. Ding, Y. B. Ou, P. Deng, K. Chang, J. Wen, C. L. Song, K. He, J. F. Jia, S. H. Ji, Y. Y. Wang, L. L. Wang, X. Chen, X. C. Ma, and Q. K. Xue, Chin. Phys. Lett. 29, 037402 (2012).

[4]. F. Nabeshima, Y. Imai, M. Hanawa, I. Tsukada, and A. Maeda, Appl. Phys. Lett. 103, 172602 (2013).

[5]. S. Y. Tan, Y. Zhang, M. Xia, Z. R. Ye, F. Chen, X. Xie, R. Peng, D. F. Xu, Q. Fan, H. C. Xu, J. Jiang, T. Zhang, X. C. Lai, T. Xiang, J. P. Hu, B. P. Xie and Donglai Feng, Nature Mater. 12, 634-640 (2013).

[6]. W. H. Zhang, Z. Li, F. S. Li, H. M. Zhang, J. P. Peng, C. J. Tang, Q. Y. Wang, K. He, X. Chen, L. L. Wang, X. C. Ma, and Q. K. Xue, Phys. Rev. B 89, 060506 (R) (2014).

[7]. R. Schneider, A. G. Zaitsev, D. Fuchs, and H. v. Löhneysen, Phys. Rev. Lett. 108, 257003 (2012).

[8]. R. Schneider, A. G. Zaitsev, D. Fuchs, and H. v. Löhneysen, Eur. Phys. J. B 88, 14 (2015).

[9]. Y. H. Lin and A. M. Goldman, Phys. Rev. Lett. 106, 127003 (2011).

[10]. R. Schneider, A. G. Zaitsev, D. Fuchs, and H. v. Löhneysen, J. Low. Temp. Phys. 178, 118-127 (2015).

[11]. E. Pomjakushina, K. Conder, V. Pomjakushin, M. Bendele, and R. Khasanov, Phys. Rev. B 80, 024517 (2009).

[12]. Y. F. Nie, E. Brahimi, J. I. Budnick, W. A. Hines, M. Jain and B. O. Wells, Appl. Phys. Lett. 94, 242505 (2009).

[13]. M. J. Wang, J. Y. Luo, T. W. Huang, H. H. Chang, T. K. Chen, F. C. Hsu, C. T. Wu, P. M. Wu, A. M. Chang, and M. K. Wu, Phys. Rev. Lett. 103, 117002 (2009).

[14]. R. Schneider, A. G. Zaitsev, D. Fuchs, and R. Fromknecht, Supercond. Sci. Technol. 26, 055014 (2013).

[15]. M. Jourdan and S. ten Haaf, J. Appl. Phys. 108, 023913 (2010).

[16]. T. M. McQueen, Q. Huang, V. Ksenofontov, C. Felser, Q. Xu, H. Zandbergen, Y. S. Hor, J. Allred, A. J. Williams, D. Qu, J. Checkelsky, N. P. Ong, and R. J. Cava, Phys. Rev. B 79, 014522 (2009).

[17]. T. K. Chen, C. C. Chang, H. H. Chang, A. H. Fang, C. H. Wang, W. H. Chao, C. M. Tseng, Y. C. Lee, Y. R. Wu, M. H. Wen, H. Y. Tang, F. R. Chen, M. J. Wang, M. K. Wu, and D. V. Dyck, Proc. Natl. Acad. Sci. U.S.A. 111, 63-68 (2014).

[18]. T. Berlijn, P. J. Hirschfeld, and W. Ku, Phys. Rev. Lett. 109, 147003 (2012).

[19]. A. S. Sefat, R. Y. Jin, M. A. McGuire, B. C. Sales, D. J. Singh, and D. Mandrus, Phys. Rev. Lett. 101, 117004 (2008).

[20]. Y. Miyata, K. Nakayama, K. Sugawara, T. Sato, and T. Takahashi, Nature Mater. 14, 775-780 (2015).

[21]. B. Lei, J. H. Cui, Z. J. Xiang, C. Shang, N. Z. Wang, G. J. Ye, X. G. Luo, T. Wu, Z. Sun, and X. H. Chen, arXiv: 1509.00620.

Table and Figures

Table 1 Detailed information of four prepared FeSe films.

	Thickness (nm)	*c*-axis(Å) bulk ~ 5.52	ΔT_c (K)	T_c^{onset} (K)	H_{c2} (T)	Fe/Se ratio (at. %)	at. % of Fe
#NS1	40	5.476	n/a	n/a	n/a	1.00:1.09	47.8%
#SC1	120	5.531	1.9	10.7	27.8	1.00:1.03	49.3%
#SC2	240	5.558	1.5	15.2	35.5	1.00:1.04	49.0%
#SC3	360	5.564	1.4	13.2	31.5	1.00:1.06	48.5%

Figure 1

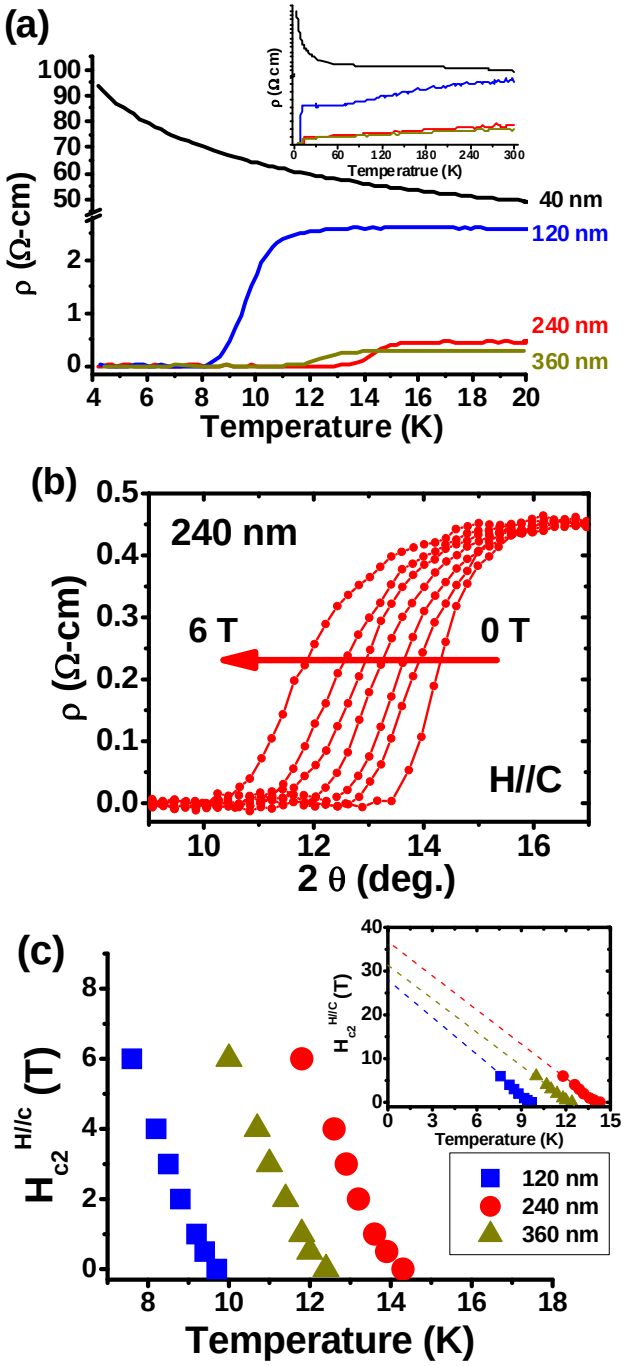

FIG. 1 (a) Temperature dependences of resistivity (R-T curves) at self-field for FeSe films with different thickness (40 nm, 120 nm, 240 nm and 360 nm) ranging from 4 K to 20 K. Inset is the full range R-T data from room temperature to 4.2 K. (b) R-T curves for FeSe film #SC2 (240 nm) under different magnetic fields up to 6 T applied along the *c*-axis. (c) Plot of upper critical field (H_{c2}) as a function of T_c^{mid} for three FeSe films showing superconductivity. The linear extrapolations to T = 0 K are shown in the inset.

Figure 2

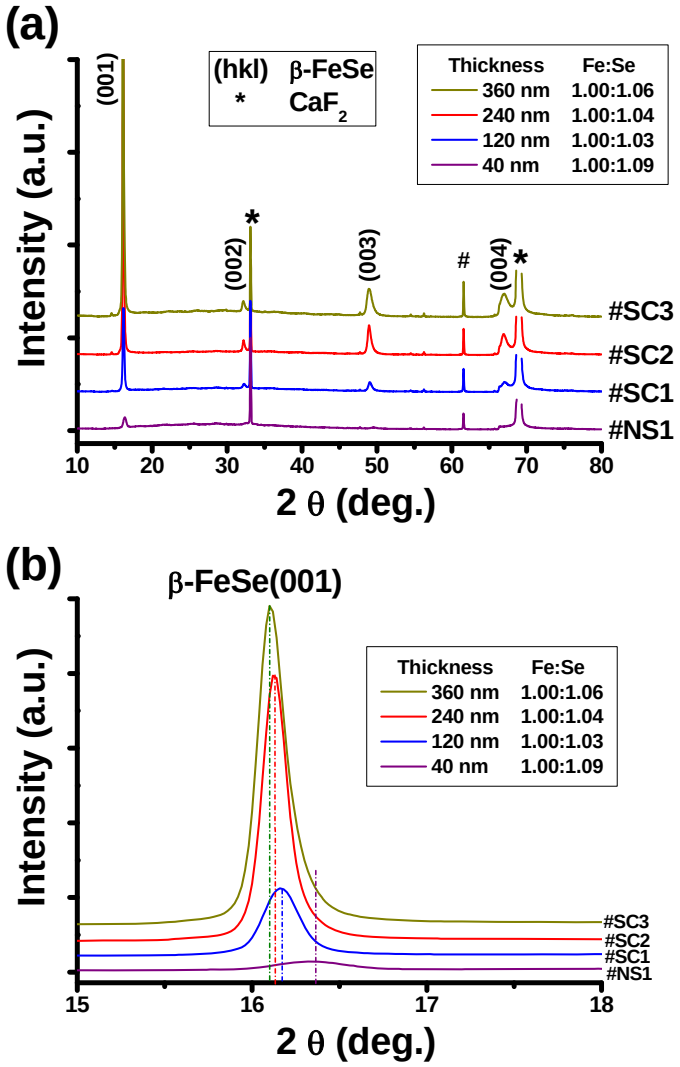

FIG. 2 (a) XRD θ-2θ patterns of four FeSe films grown on CaF_2 (100) substrate. The peaks resulting from the substrate are marked as asterisks and CaF_2 (004) peak is suppressed. The number signs represent β-FeSe peaks and the pound sign stands for unidentified peak. (b) Magnified interval between 15.5° and 17.0°, and the locations of peaks are marked by dashed lines.

Figure 3

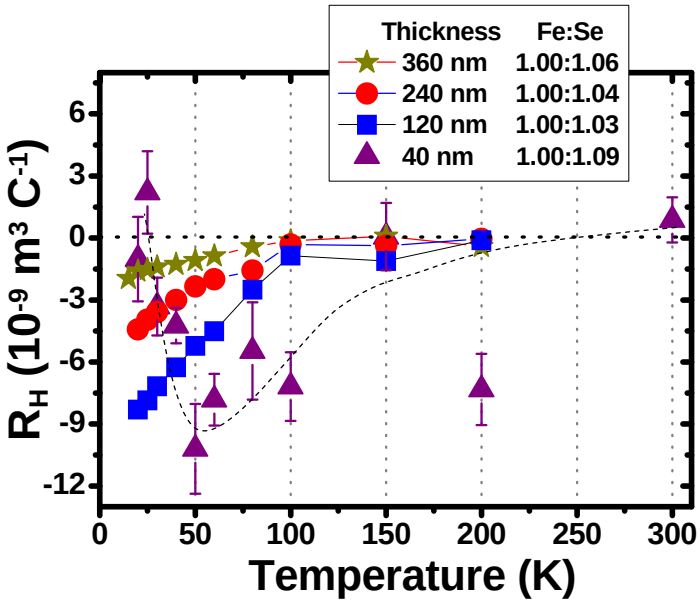

FIG. 3 Hall coefficient R_H as a function of temperature of four FeSe films. R_H is determined as $R_H = \rho_{xy}/B$, dedicating the slope of hall transverse resistivity ρ_{xy} at designated field B (> 1 T).

Figure 4

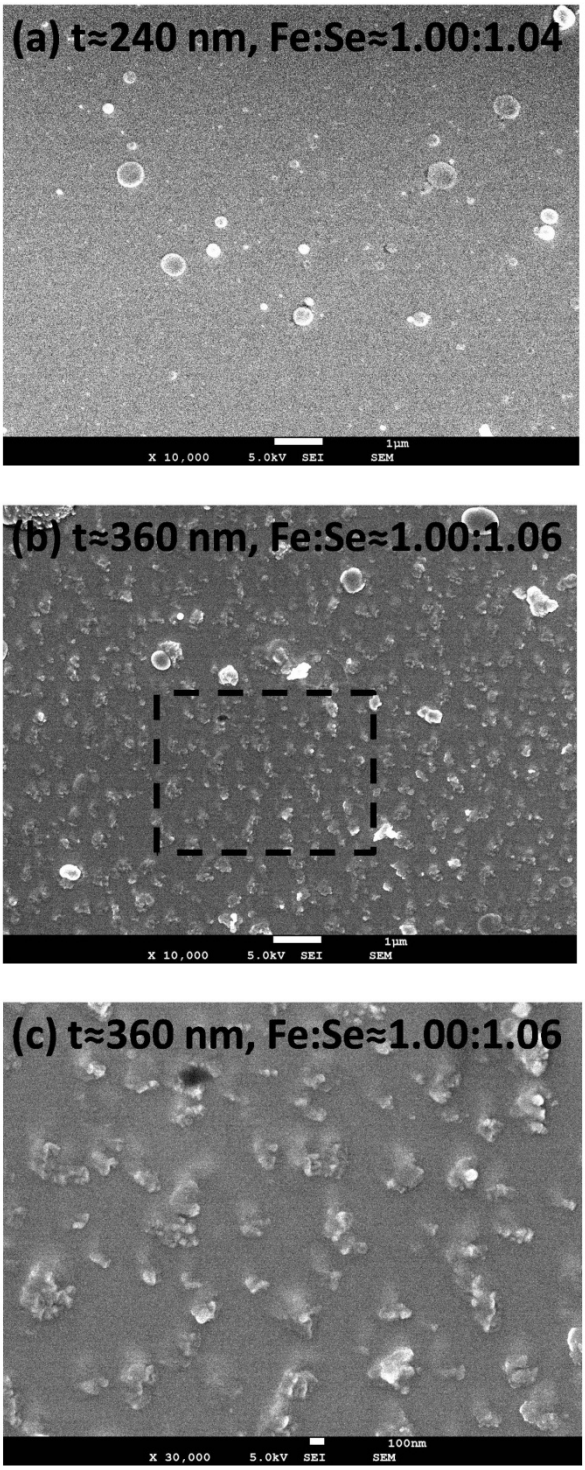

FIG. 4 Scanning electron micrographs of FeSe films with (a) #SC2, Fe:Se ≈ 1.00:1.04, (b) #SC3, Fe:Se ≈ 1.00:1.06 and (c) Enlarged image of the rectangular region in (b) for checking the precipitates generated on the surface of FeSe film.